Supporting Information

Clean rhodium nanoparticles prepared by laser ablation in liquid for high performance electrocatalysis of the hydrogen evolution reaction

Giulia Alice Volpato,[1] David Muneton Arboleda,[2] Riccardo Brandiele,[1] Francesco Carraro,[1] Giovanni Battista Sartori,[1] Andrea Cardelli,[1] Denis Badocco,[1] Paolo Pastore,[1] Stefano Agnoli,[1] Christian Durante,[1,*] Vincenzo Amendola,[1,*] Andrea Sartorel[1,*]

[1] Department of Chemical Sciences, University of Padova, via Marzolo 1, 35131 Padova (Italy).
[2] Centro de Investigaciones Ópticas CIOp (CONICET-CIC- UNLP) and Facultad de Ingeniería UNLP, La Plata, Argentina
* christian.durante@unipd.it; vincenzo.amendola@unipd.it; andrea.sartorel@unipd.it

SUMMARY

Experimental

NPs synthesis and characterization

The LASiS was performed using 1064 nm (6 ns, 50 Hz) pulses of a Nd-YAG laser focused with a 10 cm lens up to a fluence of 7.6 J/cm^2 on a Rh 99.99% pure rod (from Mateck) placed at the bottom of a cell containing either distilled water or HPLC grade ethanol (from Sigma Aldrich). Then, the so obtained Rh NPs dispersions were collected by centrifugation (3000 rcf for 30 min), washed several times with HPLC grade ethanol and, finally, redispersed in HPLC grade ethanol, at a final concentration of 0.112 mg_{Rh}/mL for E-Rh NPs and 0.075 mg_{Rh}/mL for W-Rh NPs. The difference in Rh concentration between the two samples reflects the difference in the ablation time, that in a typical synthesis was 2 h in ethanol and 1 h in water.

Rh concentration was assessed by inductively coupled plasma-mass spectrometry (ICP-MS) with an Agilent Technologies 7700x ICP-MS (Agilent Technologies International Japan, Ltd., Tokyo, Japan). In order to correctly digest the NPs samples, 100 mg of the analyte were dissolved in 3 g of 69 % HNO_3 and 3 g of HCl 37% heated for 30 min at 100 °C with a microwave digester CEM EXPLORER SP-D PLUS. After cooling, solutions were diluted in order to obtain Rh concentration in the required calibration range and in 5 % w/w aqua regia solution.

TEM analysis was performed with a FEI Tecnai G2 12 transmission electron microscope operating at 100 kV and equipped with a TVIPS CCD camera. High-resolution TEM, SAED, and EDS analysis were performed at 300 kV using a JEOL JEM 3010 TEM using a Gatan Multiscan CCD 794 and EDS (Oxford Instruments). The samples for TEM analysis were prepared by evaporating NP suspensions on a copper grid coated with an amorphous carbon holey film.

Raman measurements were recorded using a Renishaw inVia micro-Raman spectrometer on a dried powder of W-Rh-NPs or E-Rh-NPs, using the 633-nm line (1 mW) of a He–Ne laser and a 20X objective.

Photoemission spectra were acquired in a custom designed UHV system equipped with a hemispherical electron analyser (Omicron EA125) and a dual anode Al/Mg non monochromated source (Omicron DAR400), working at a base pressure of $2x10^{-10}$ mbar. The binding energy scale was calibrated positioning the Au 4f level core levels of a Au(111) sample at 84 eV. Small portions of copper electrodes bearing the ink were measured prior and after the electrochemical work. All spectra were acquired with the Mg Kα emission line (1253.6 eV) at room temperature after degassing the sample overnight using a pass energy of 20 eV. The deconvolution into chemically shifted components was performed by means of Voight functions after subtracting a Shirley background. Since the photoemission spectra have been acquired directly in the ink used for the catalytic tests in order to identify possible chemical changes as a consequence of the electrochemical work, the analysis of the O 1s spectra is quite difficult, because the signal form Rh oxide is overlapped to that of the oxygen species coming from the ink components (i.e. carbon support, nafion, water, propanol). For this reason, these data were omitted.

The morphology of the materials was investigated using a scanning electron microscopy SEM (Zeiss Supra VP35) equipped with an Oxford energy-dispersive x-ray spectroscopy (EDX) microprobe.

Electrochemistry

Electrochemical characterizations were performed in a three-electrodes configuration in air-tight heart-shaped electrochemical cells using a BioLogic SAS SP-300 potentiostat/galvanostat (voltammetry, Electrochemical Impedance Spectroscopy) and an Amel Instruments – 7050 potentiostat/galvanostat (chronopotentiometry).

The electrolytes were purged with N_2 or Ar before each measure. When reference electrodes other than the Reversible Hydrogen Electrode were employed during an experiment, the potentials were subsequently converted to RHE. The RHE was freshly prepared before each experiment and consists in a Pt wire mesh sealed to the closed end of a capillary glass tube and filled with the electrolyte solution from the other open end; H_2 was directly electrogenerated at the Pt wire mesh so that half of the Pt mesh was exposed to H_2 contained in the upper part of the capillary. A Hg/HgO reference electrode (MMO) was used in 0.1 M KOH.

When reported, the compensation of the solution resistance was automatically performed during the measures employing the potentiostat feedback system. The solution resistance was previously obtained from the Nyquist plot resulting from Electrochemical Impedance Spectroscopy (EIS) measures performed at OCP in the frequency range 200 kHz – 100 mHz (sinus amplitude = 5 mV, 6 points per decade, 3 measures per frequency). The percentage of compensation was always fixed at 85% to avoid overcompensation. The solution resistance was 4 Ω and 7.5 Ω in 0.1 M H_2SO_4 and 6.2 Ω and 8.4 Ω in 0.1 M KOH, for W-Rh/C and for E-Rh/C, respectively.

Calibration MMO to RHE. The calibration of Hg/HgO electrode was performed in a standard three electrode cell with Pt wires as the working and counter electrodes, and the Hg/HgO (MMO) electrode as the reference electrode. Electrolyte was purged and saturated with high purity H_2. Linear scanning voltammetry (LSV) was recorded at a scan rate of 0.5 mV s−1 between -0.9 V vs MMO and -1 V vs MMO, and the potential at which the current crossed zero is taken to be the thermodynamic potential for the hydrogen electrode reactions.

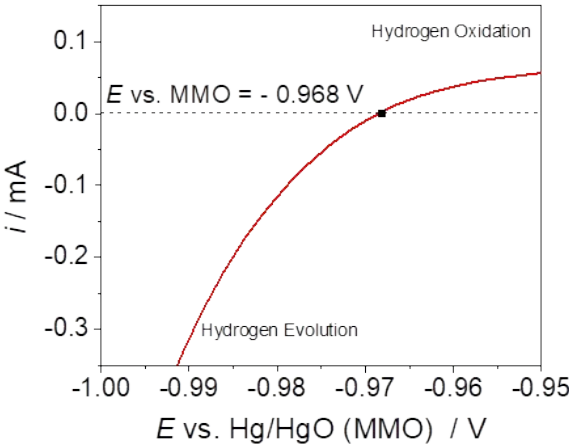

Preparation of working electrodes. The suspensions of E/W-Rh NPs in ethanol were mixed with mesoporous carbon black (Vulcan XC-72 from Fuel Cell Store) by sonication, maintaining a metal/carbon ratio close to 30/70; 0.02% w/w Nafion (from 5% Nafion solution in propanol) was added to ensure mechanical stability of the dried ink; 37% v/v water was added to the ink solution in order to increase the surface tension of the ink droplets, thus achieving a better control of the deposition area. More specifically, the amount of Vulcan, Rhodium and Nafion were fixed at 0.9 mg, 0.4 mg and 6 µL for both the inks: given the different metal content in the starting NPs suspensions (0.112 mg_{Rh}/mL for E-Rh NPs, 0.075 mg_{Rh}/mL for W-Rh NPs), the density of E-Rh/C and W-Rh/C inks were 70 μg_{Rh}/mL and 47 μg_{Rh}/mL, respectively. The Pt/C ink used for comparison was prepared from commercial Pt/C (Platinum on carbon black, HiSPEC® 7000 from Alfa Aesar – Pt NPs with 4-7 nm diameter, Pt/carbon ratio of 30/70), maintaining the same conditions used for Rh NPs inks.

Glassy carbon electrodes (GCE) were polished using diamond paste (from Struers - 3 µm, 1 µm and 0.25 µm), sonicated in milliQ water and then in ethanol. Teflon tape masks were used to cover the insulating coating of the GCE during the deposition of the ink. The ink suspensions, previously sonicated for 1 hour, were deposited onto electrodes by repeatedly drop-casting 5 µL of ink to obtain a final metal loading of 20 µg/cm^2 and dried in air at room temperature overnight. A 0.5x0.5 cm^2 active area was created when depositing the inks on carbon paper.

Determination of Electrochemical Surface Area (ESA). The stripping of the adsorbed CO monolayer was used for the determination of the active surface area of Rh/C and Pt/C in 0.5 M H_2SO_4. CO was bubbled into the

Ar purged electrolyte, while applying a constant potential of 0.1 V vs RHE to the electrodes, in order to activate the sites involved in HER, thus allowing the binding of one CO monolayer. After 10 minutes, the electrolyte was purged again with Ar for 40 minutes to eliminate unadsorbed CO, while keeping the potential at 0.1 V. The potential was then cycled between 0.1 and 1.4 V *vs* RHE (20 mV/s) to achieve the oxidation of adsorbed CO.[1,2] Given the partial superimposition between the Rh(I) → Rh(III) peak at E_{pa} = 0.7 V vs RHE and the CO oxidation region (0.8 - 1.2 V vs RHE), the CV recorded before the exposure to CO was previously subtracted to the CO stripping voltammogram and the resulting curve was then integrated between 0.8 V and 1.2 V vs RHE. The electrochemical surface area (ESA) was then calculated with the following equation:

$$ESA = \frac{S}{\nu \cdot c}$$

where S is the integrated area of the CO-stripping region, ν is the scan rate and c is the charge required to oxidize one CO monolayer on Rh surface (420 μC/cm²). The electrochemical active surface area (ECSA) was then calculated by dividing the ESA for the metal loaded on the GCE (0.071 cm² geometric surface area).

Determination of turnover frequency (TOF).

TOF has been calculated from the equation:

$$TOF\ (s^{-1}) = \frac{J}{2 \times F \times n}$$

where J is the current density (in A/cm²) at a defined potential, F is the Faraday constant (96485C/mol), n is the Rh total surface loading (in mol/cm²).[9]

Electrochemical Impedance Spectroscopy. EIS was performed in 0.1 M H_2SO_4, at potentials between +20 mV and -40 mV vs RHE (10 mV steps) in the 2 MHz – 20 mHz frequency range (2 measures per each frequency, 6 points per decade), using a potential amplitude of 5 mV.

Chronopotentiometry and Faradaic Yield determination. Chronopotentiometries were performed at -10 mA/cm² in a H-shaped electrochemical cell to separate cathodic and anodic compartment. Working electrode: inks deposited onto GCE (3 mm diameter, geometric surface area = 0.0706 cm²) or carbon paper (geometric surface area = 0.250 cm²); counter electrode: Pt mesh; reference electrode: Ag/AgCl (3M NaCl); no iR drop compensation. The 0.1 M H_2SO_4 electrolyte in both the compartments was purged with N_2 for 1 hour.

The quantification of hydrogen evolved during galvanostatic experiments was performed by means of a Agilent 7890A gas chromatographer, equipped with a HP-MOLSIEVE column (60 m x 320 μm x 20 μm), coupled to a thermal conductivity detector (TCD), manually sampling the headspace of the cathodic compartment: Ar was used as gas carrier; since N_2 amount in the headspace can be considered constant, the N_2 peak in the TCD chromatogram was used as internal standard; the hydrogen amount was then calculated from the H_2 to N_2 integrated areas ratio multiplied by the H_2 TCD-response factor (116 ± 3 μmol_{H2}) obtained by previous calibration (see Figure on the right).

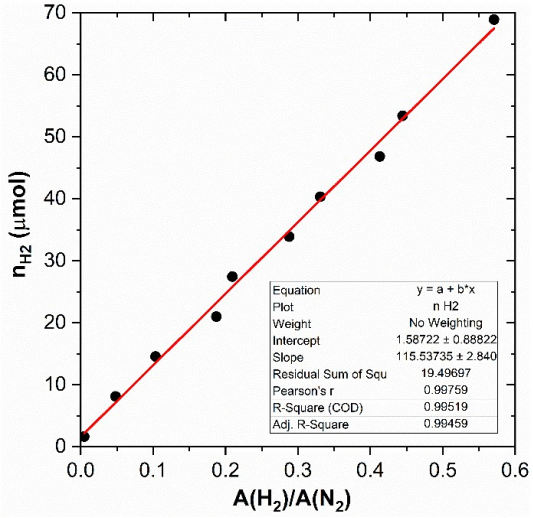

The GC-TCD calibration for H_2 was performed with a galvanostatic experiment at -2 mA with a Pt mesh WE in 0.1 M H_2SO_4, in a H-shaped cell: the charge corresponding to each sampling of the headspace was converted in moles of hydrogen, n_{H2}, assuming 100% Faradaic Yield, and then plotted against the corresponding H_2 to N_2 integrated areas ratio, $A(H_2)/A(N_2)$, calculated from the TCD chromatogram.

The details of the GC-TCD method are reported in the following table:

Flow	Oven	TC Detector	Other
Gas carrier: Ar	Initial T: 70°C	T: 200°C	Injected volume: 200 µL
Total Flow: 82.98 mL/min	Initial time: 18 min	Make-up flow: 6 mL/min	t =18 – 25 min: column excluded
Flow Splitting: 20:1	Ramp: 15°C/min	Reference flow: 15 mL/min	H_2 retention time: 7.6 min
Column Flow: 4.81 mL/min	Final T: 170°C	Filament: 25 µV	N_2 retention time: 9.6 min
Column pressure: 45 psi	Final time: 1 min		

Supplementary Figures and Tables

Table S1. Summary and benchmarking of the main results obtained with carbon supported E-Rh NPs and W-Rh NPs as HER catalysts **in acidic environment**.

SYSTEM	Electrolyte	M load.	ECSA	Tafel slope	η (mV) @ J_{geom} (mA/cm²) [c]			SA @ -50 mV	MA@ -50 mV	Ref.
		(μg/cm²)	(m²/g)	(mV/dec)	-1	-5	-10	(mA/cm²$_M$)	(mA/μg$_M$)	
W-Rh/C	0.1 M H_2SO_4	20	65 ± 7	50.2 ± 0.1[a] (50 ± 3)[b]	-16 ± 1	-41 ± 2	-57 ± 1	1.69 ± 0.06	0.390 ± 0.004	This work
E-Rh/C			48 ± 9	54.3 ± 0.2 [a] (42 ± 2)[b]	-32 ± 4	-75 ± 9	-110 ± 10	0.7 ± 0.1	0.130 ± 0.005	
Comm. Pt/C			270 ± 10	48.4 ± 0.3 [a]	-1.6 ± 0.6	-7.8 ± 0.5	-11 ± 1	0.44 ± 0.03 [d]	0.42 ± 0.03 [d]	
coarse Rh NWs	0.1 M H_2SO_4	-	-	23	-	-	-	0.33	-	[3]
smooth Rh NWs			-	33	-	-	-	0.09	-	
Rh-Rh_2O_3-NPs/C	0.5 M H_2SO_4	28	35	32	-	-	-13	9.6 [e]	3.4 [e]	[4]
Comm. Rh/C			15	50	-	-	-55	6.2	1.0	
Comm. Pt/C			42	34	-	-	-24	5.6	2.3	
Rh/SiQD/CQD-3	0.5 M H_2SO_4	9	16.5	26	-	-	-36 [f]	13.5	2.5	[5]
5 nm Rh NCs/C	0.5 M H_2SO_4	13.3	-	-	-16 [f]	-68.4 [f]	-	-	-	[6]
5 nm Rh_2P NCs/C		3.7	-	-	+14	-5.4	-	-	-	
29%wt Rh NPs/Si NWs [g]	0.5 M H_2SO_4	56	-	24 [e]	-	-	-84 [f]	-	-	[7]
Rh NPs [h]		193	-	40	-	-	-129	-	-	

[a] Tafel slope derived from RDE-LSV at 0.5 mV/s and [b] Tafel slope derived from chronoamperometries. [c] Overpotential necessary to reach current densities of -1 mA/cm², -5 mA/cm² or -10 mA/cm². The values reported in acid are averaged over two samples and over two consecutive LSV scans. [d] SA and MA values at -10 mV of overpotential. [e] SA and MA values at -100 mV of overpotential. [f] Scan rate of 5 mV/s. [g] Co-catalytic system obtained by growing Rh NPs onto Si NWs; [h] Rh NPs obtained upon removal of the Si NWs by etching.

Table S2. Summary and benchmarking of the main results obtained with carbon supported E-Rh NPs and W-Rh NPs as HER catalysts **in alkaline environment**.

SYSTEM	Electrolyte	M load.	ECSA	Tafel slope	η (mV) @ J_{geom} (mA/cm²) [a]			SA @ -0.1 V	MA@ -0.1 V	Ref.
		(μg/cm²)	(m²/g)	(mV/dec)	-1	-5	-10	(mA/cm²$_M$)	(mA/μg$_M$)	
W-Rh/C	0.1 M KOH	20	65 ± 7	41 ± 1 [b]	-1.0 ± 0.1 (-13 ± 1)	-64 ± 1 (-73 ± 2)	-113 ± 4 (-123 ± 4)	1.89	0.44	This work
E-Rh/C			48 ± 9	44.0 ± 0.4[b]	-21 ± 1 (-30 ± 1)	-97 ± 4 (-114 ± 3)	-157 ± 8 (-176 ± 8)	1.49	0.26	
Rh-Rh_2O_3-NPs/C	0.5 M KOH	28	28	70		-	-63	2.56	0.72	[4]
Comm. Rh/C			12	116		-	-150	1.45	0.17	
Comm. Pt/C			38	113		-	-103	0.87	0.33	
(18.4x4 nm) Rh NSs/C [c]	0.1 M KOH	15.3	65.3	80 [e]		-19 [e]	-37	3.5	1.8	[8]
(3.3 nm) Rh NCs/C [d]		15.3	32.15	75		-41	-	3.7	1.2	
Comm. Rh/C		-	36.3	118		-37	-	2.2	0.7	

[a] Overpotential necessary to reach current densities of -5 mA/cm². Since a decrease in performance was observed between consecutive scans in alkaline environment, the two reported values refer to the average over two samples for the first and second (between bracket) scan, respectively. [b] Tafel slope derived from LSV at 2 mV/s [c] Rh nano-sheets and [d] tetrahedral Rh nano-crystals; [e] scan rate of 10 mV/s.

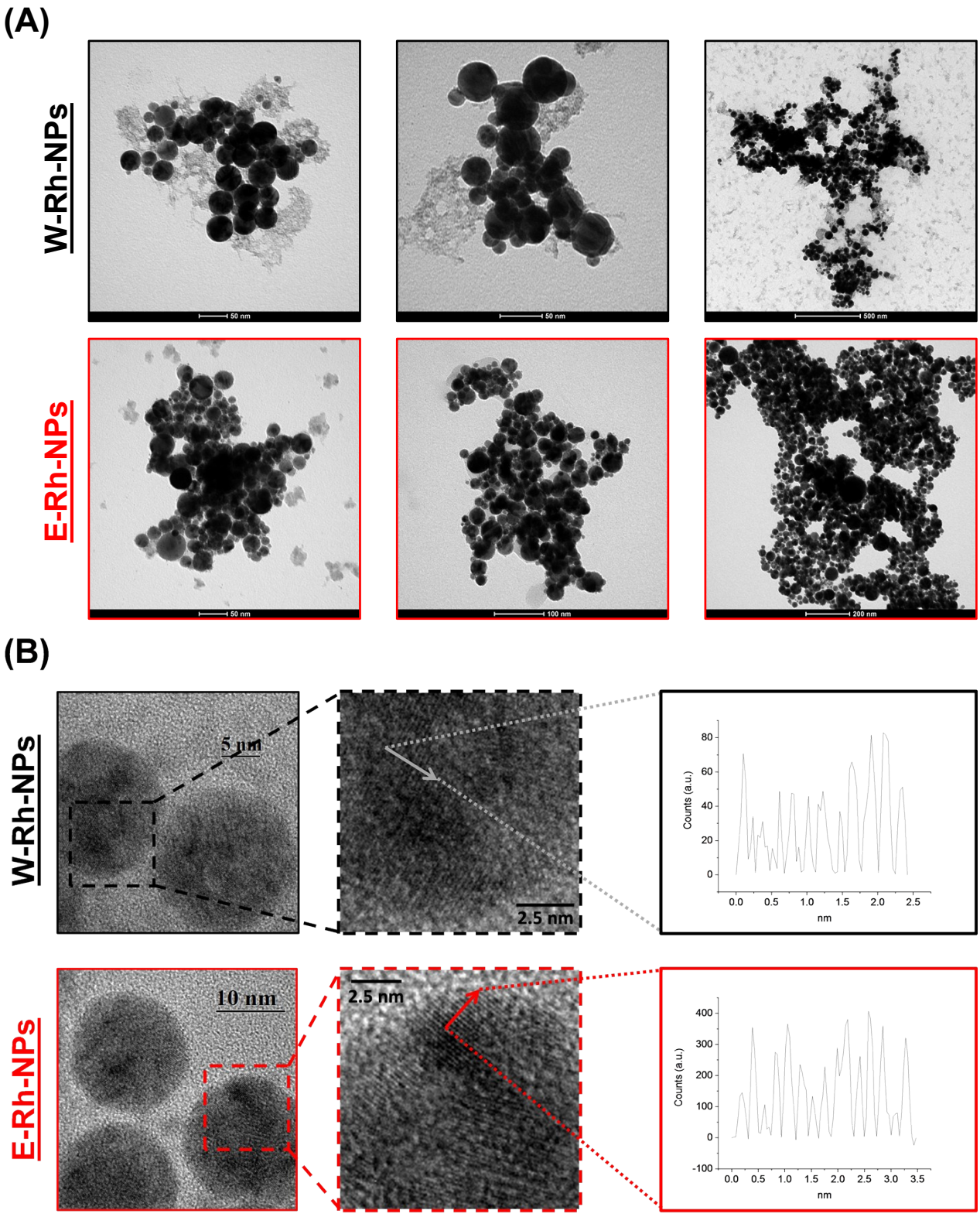

Figure S1. (A) Additional TEM images of W-Rh/C (top) **and E-Rh/C** (bottom) NPs. **(B) HRTEM images** of **W-Rh/C** (top) **and E-Rh/C** (bottom) NPs showing lattice fringes inside small (few nm) crystalline domains embedded in a highly defective and polycrystalline structure. The projection of the bright field image intensity along a linear path perpendicular to the lattice fringes is also reported on the right.

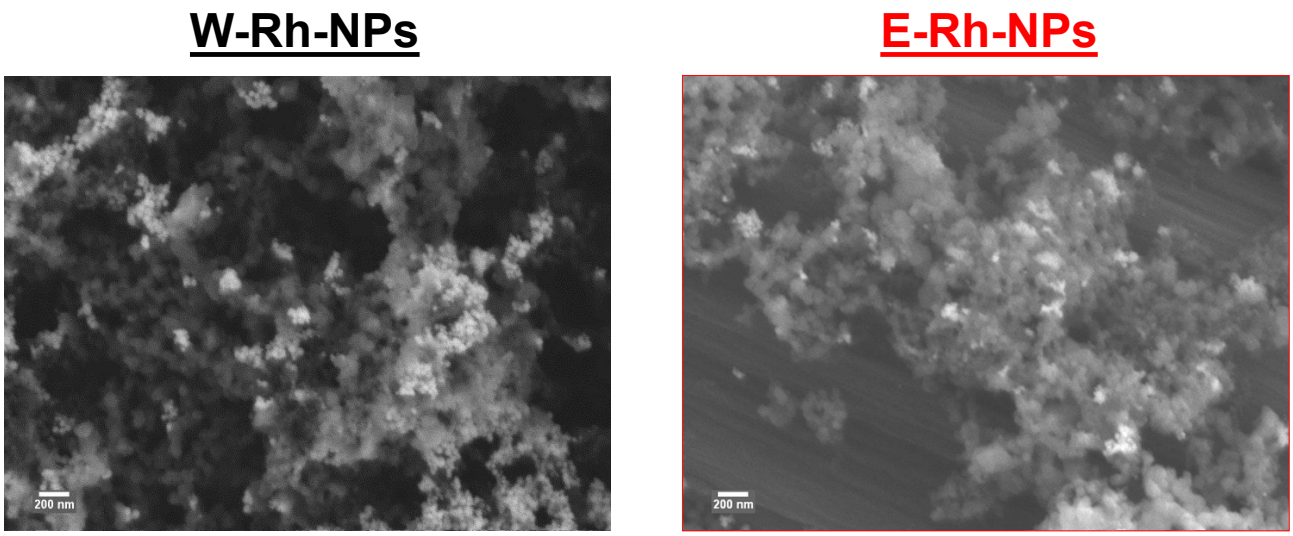

Figure S2. SEM of **W-Rh/C** (left) and **E-Rh/C** (left) inks supported onto carbon paper (20 μg Rh/cm^2).

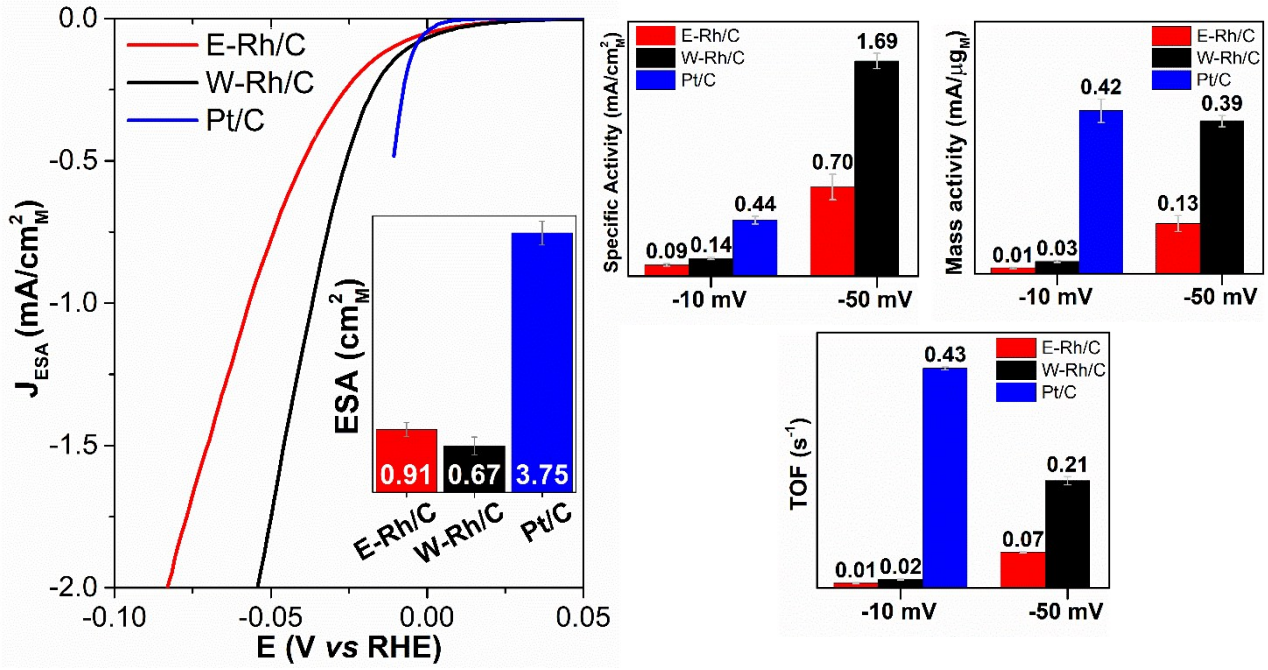

Figure S3. Left) Linear sweep voltammograms in 0.1 M H_2SO_4 (2 mV/s, 85% iR drop compensation) of E-Rh/C, W-Rh/C and Pt/C (20 μg metal/cm^2) supported onto GCE (0.196 cm^2 geometric area), with current normalized for the electrochemical surface area (ESA). Inset: Electrochemical Surface Areas (ESA) of the catalysts. **Right)** Specific activity, mass activity and turnover frequency of E-Rh/C, W-Rh/C and comm. Pt/C at -10 mV and -50 mV of overpotential.

The specific activity refers to the value of J_{ESA} at a certain overpotential. The mass activity was calculated by dividing the geometric current density for the metal loading.

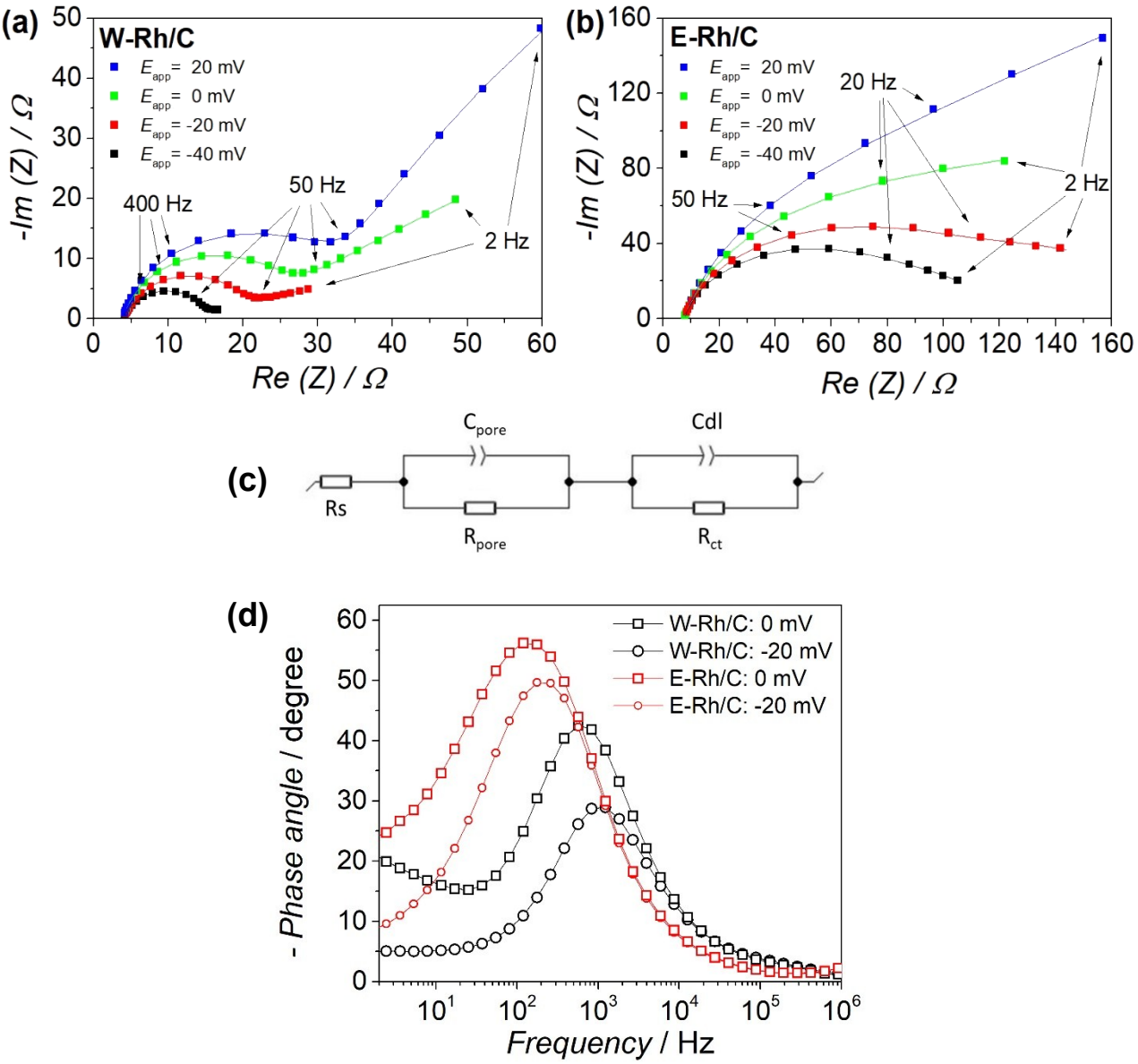

Figure S4. EIS measurements for E-Rh/C and W-Rh/C inks (20 μg Rh/cm^2) supported onto GCE (0.196 cm^2 geometric area) in 0.1 M H_2SO_4, plotted in the 1 MHz – 2 Hz range. Nyquist plots for W-Rh/C **(a)** and E-Rh/C **(b)** recorded at applied potentials of 20 mV, 0 mV, -20 mV and -40 mV vs RHE. **(c)** The modified Randles equivalent circuit employed for data fitting. **(d)** Bode plots for W-Rh/C and E-Rh/C recorded at applied potentials of 0 mV (square) and -20 mV (circles) vs RHE.

The Nyquist plots show the presence of a semicircle and a non-ideal diffusion zone which are connected to charge transfer process of HER and to the nanoparticle surface textural properties, respectively. For both the samples, the charge transfer resistance, $R_{CT,}$ decreases with the decrement of the applied potential. For E-Rh/C, the semicircle at low frequencies appears only at more negative potentials in comparison to W-Rh/C, consistently with the presence of a carbon capping layer which increases the material resistance and reduces the charge transfer due to the partial shielding of the Rh NPs active sites.[5] The data were fitted employing a modified Randles equivalent circuit, suggested in literature for similar systems [5] and reported in panel **(c)**.

The time constants for charge transfer were calculated from the frequency associated to the maximum vertex in the Bode plot, with the following equation:

$$\tau_{CT} = (2\pi f^{max})^{-1}.$$

The results are reported in **Table S3**. W-Rh/C shows a faster charge transfer with respect to E-Rh/C, as proved by the lower charge transfer impedances and time costants.

On the base of the parameters of the equivalent circuit, the real surface area was calculated to be 1.04 cm^2 for W-Rh/C and 0.76 cm^2 for E-Rh/C,[5] which are in agreement with the ESA evaluated by CO stripping, 0.91 cm^2 and 0.67 cm^2.

Table S3. Results of **the EIS analyses** performed for **E-Rh/C** and **W-Rh/C in 0.1 M H_2SO_4.**

			Applied potential vs RHE			
			20 mV	**0 mV**	**-20 mV**	**-40 mV**
W-Rh/C	**Fitting parameters**	**R_S (Ω)**	3.972	3.570	3.462	3.433
		C_{dl} (F)	$6.41 \cdot 10^{-5}$	$4.80 \cdot 10^{-5}$	$4.46 \cdot 10^{-5}$	$3.20 \cdot 10^{-5}$
		R_{CT} (Ω)	**27.26**	**17.86**	**13.02**	**11.29**
		R_{pore} (Ω)	295.1	279.2	55.43	9.032
		C_{pore} (F)	$2.01 \cdot 10^{-3}$	$1.12 \cdot 10^{-2}$	$3.29 \cdot 10^{-2}$	$5.74 \cdot 10^{-2}$
	τ_{CT} (ms)		**0.281**	**0.281**	**0.191**	**0.129**
E-Rh/C	**Fitting parameters**	**R_S (Ω)**	7.434	7.435	7.509	7.420
		C_{dl} (F)	$2.03 \cdot 10^{-4}$	$9.99 \cdot 10^{-5}$	$8.29 \cdot 10^{-5}$	$7.27 \cdot 10^{-5}$
		R_{CT} (Ω)	**407.9**	**126.5**	**85.42**	**63.53**
		R_{pore} (Ω)	255.3	237.9	91.94	53.8
		C_{pore} (F)	$1.25 \cdot 10^{-4}$	$6.77 \cdot 10^{-4}$	$8.29 \cdot 10^{-4}$	$1.30 \cdot 10^{-3}$
	τ_{CT} (ms)		**1.331**	**1.331**	**1.026**	**0.902**

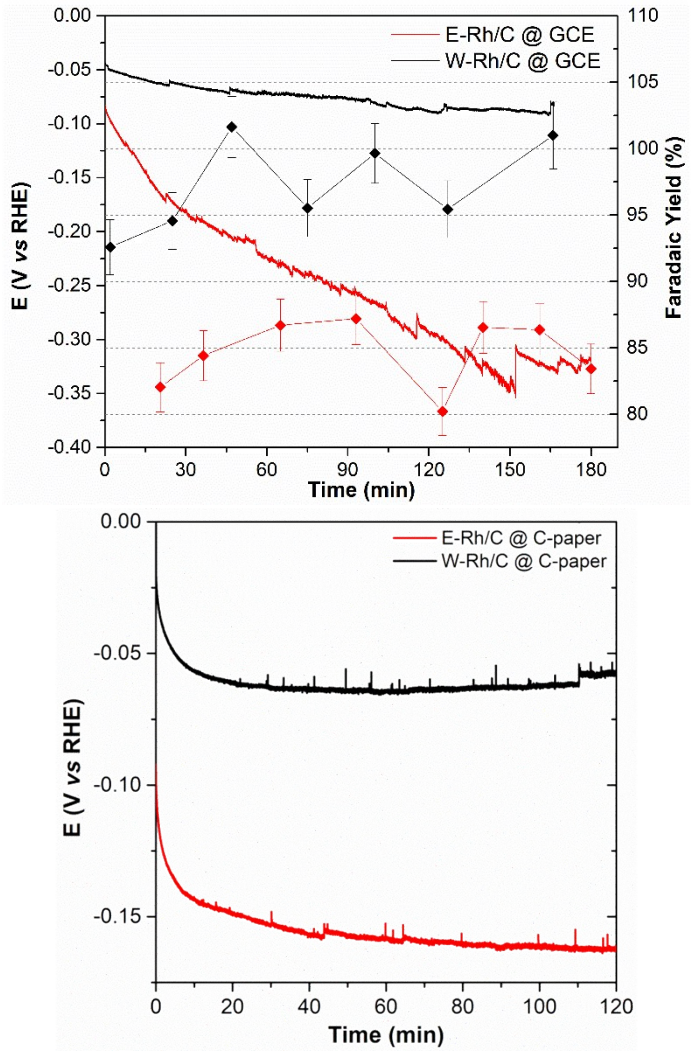

Figure S5. Chronopotentiometry of E-Rh/C and W-Rh/C inks (20 µg Rh/cm^2) supported onto GCE **(top)** or carbon paper **(bottom)** at -10 mA/cm^2 (J_{geom}) in 0.1 M H_2SO_4, coupled to quantification by GC-TCD of faradaic yield for H_2 (right Y-axis). The initial shift of the operating potentials towards more negative values can be ascribed to the initial formation of bubbles at the electrode.

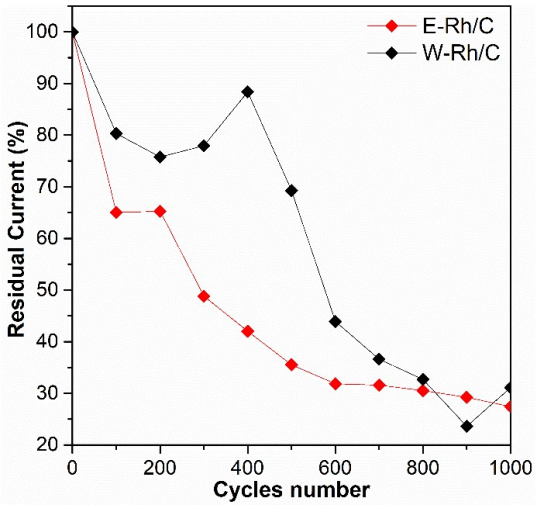

Figure S6. Stress test: residual current registered at -0.45 V vs RHE with increasing number of voltammetric cycles (+0.2 V – -0.45 V, 100 mV/s, no iR drop compensation) in 0.1 M H_2SO_4. The measure consisted of 10 separate sets of 100 cycles, with the electrolytic solution stirred for 1 minute in between each set: the data points reported in the graph correspond to the first scan of each set.

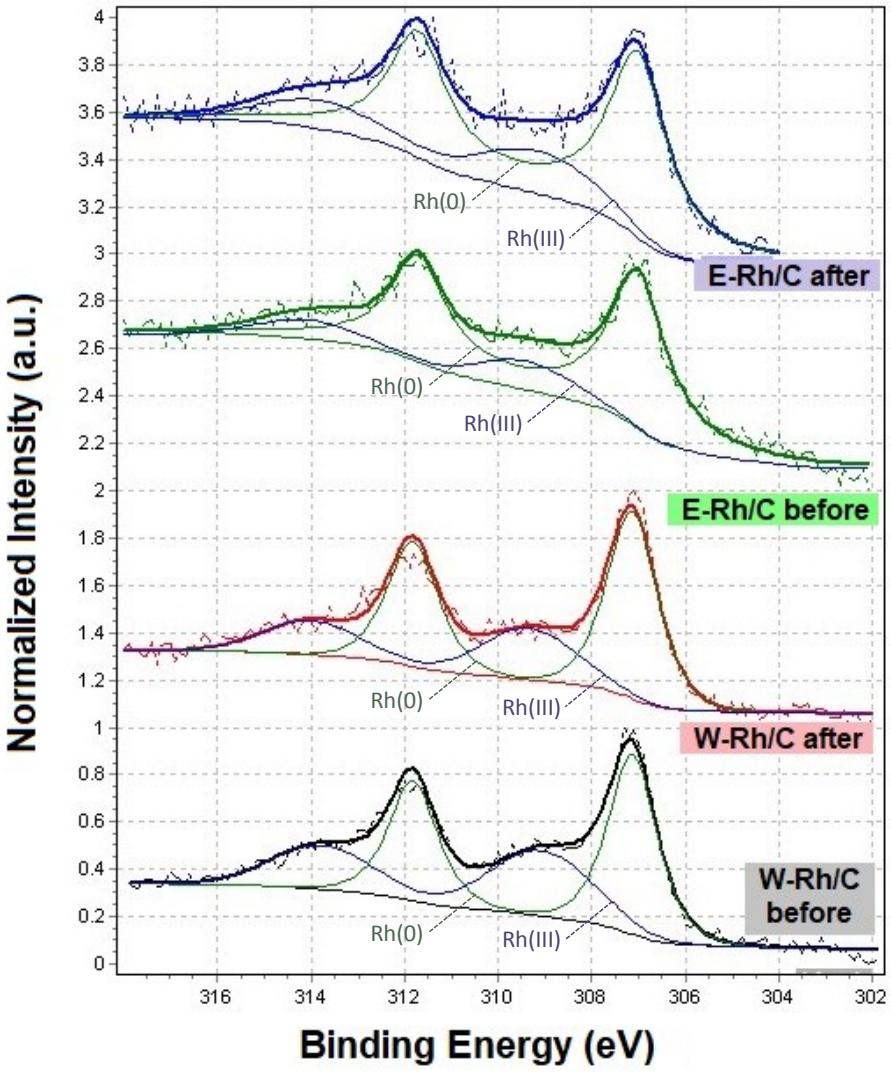

Figure S7. XPS of E-Rh/C and W-Rh/C inks supported onto carbon paper (20 µg Rh/cm^2), before and after 2-hour chronopotentiometry at -10 mA/cm^2 in 0.1 M H_2SO_4.

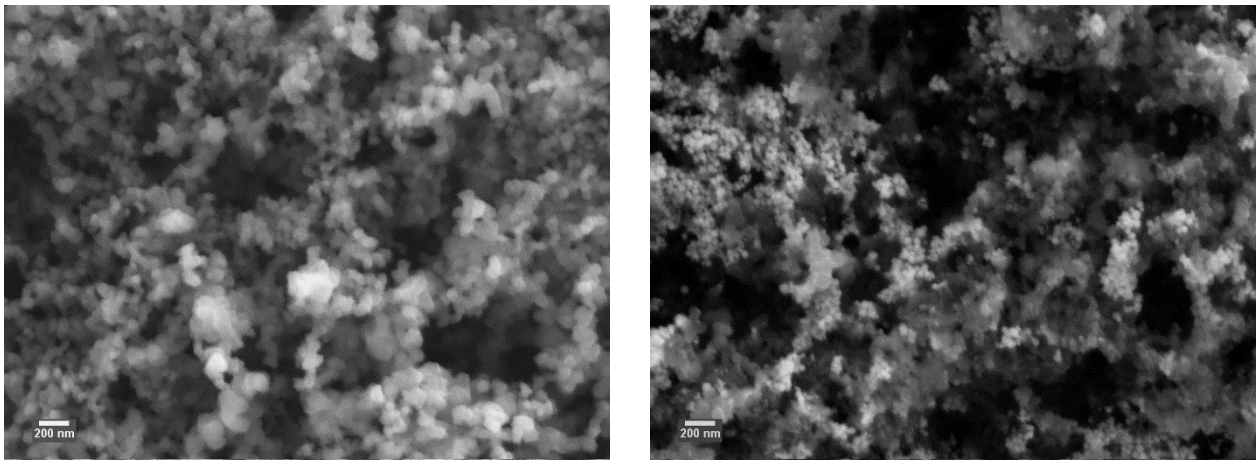

Figure S8. SEM of E-Rh/C (left) **and W-Rh/C** (right) inks supported onto carbon paper (20 µg Rh/cm^2), after 2-hour chronopotentiometry at -10 mA/cm^2 in 0.1 M H_2SO_4.

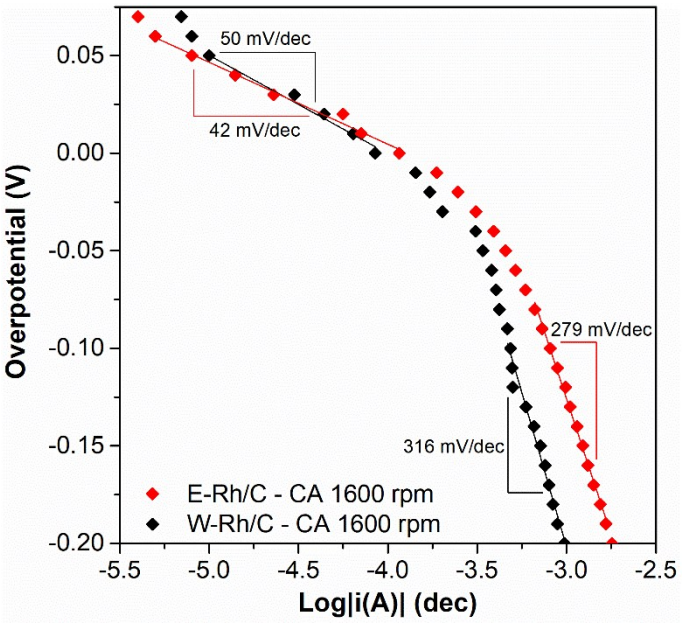

Figure S9. Tafel plot of E-Rh/C and W-Rh/C inks deposited onto GCE in 0.1 M H_2SO_4, obtained from chronoamperometries with RDE at 1600 rpm.

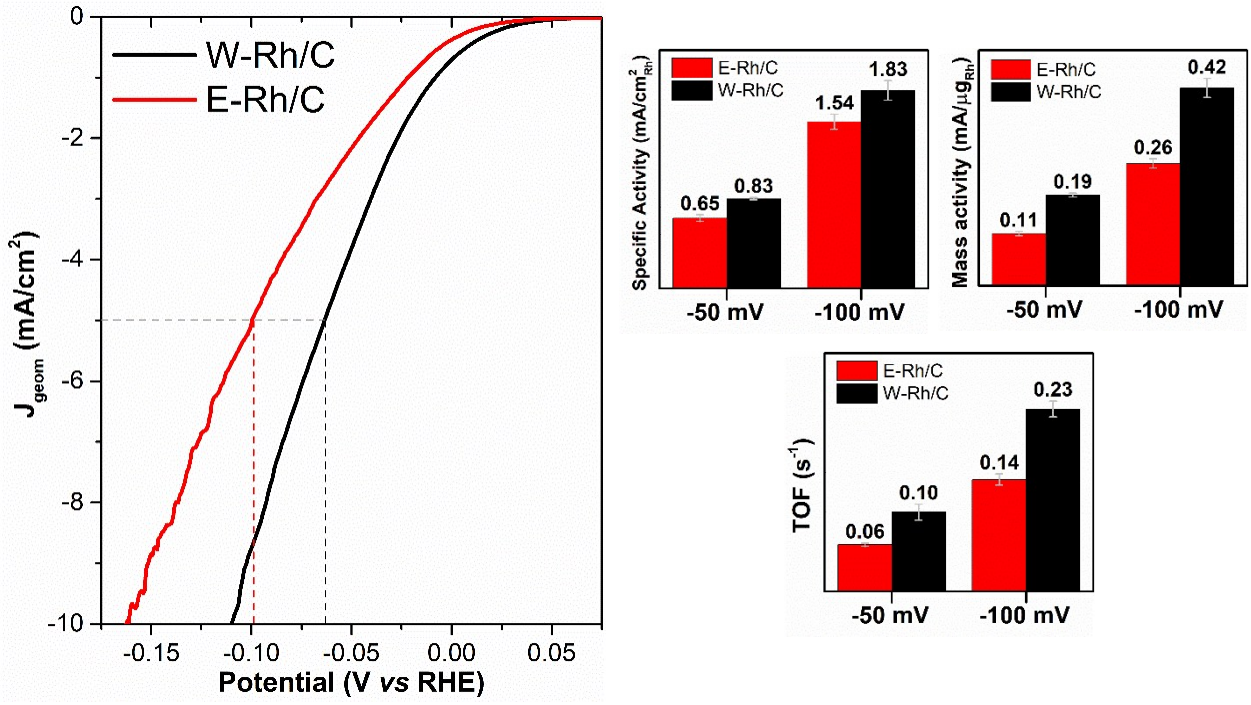

Figure S10. Left) Linear sweep voltammograms in 0.1 M KOH (2 mV/s, 85% iR drop compensation) of E-Rh/C and W-Rh/C supported onto GCE (0.196 cm^2 geometric area) with a metal loading of 20 μg/cm^2. **Right)** Specific activity, mass activity and turnover frequency of E-Rh/C, W-Rh/C at -50 mV and -100 mV of overpotential.

References

(1) Housmans, T. H. M.; Feliu, J. M.; Koper, M. T. M. CO Oxidation on Stepped Rh[n (1 1 1) × (1 1 1)] Single Crystal Electrodes: A Voltammetric Study. *J. Electroanal. Chem.* **2004**, *572* (1), 79–91.

(2) Yu, N. F.; Tian, N.; Zhou, Z. Y.; Huang, L.; Xiao, J.; Wen, Y. H.; Sun, S. G. Electrochemical Synthesis of Tetrahexahedral Rhodium Nanocrystals with Extraordinarily High Surface Energy and High Electrocatalytic Activity. *Angew. Chemie - Int. Ed.* **2014**, *53* (20), 5097–5101.

(3) Zhang, L.; Liu, L.; Wang, H.; Shen, H.; Cheng, Q.; Yan, C.; Park, S. Electrodeposition of Rhodium Nanowires Arrays and Their Morphology-Dependent Hydrogen Evolution Activity. *Nanomaterials* **2017**, *7* (5), 103.

(4) Kundu, M. K.; Mishra, R.; Bhowmik, T.; Barman, S. Rhodium Metal–Rhodium Oxide (Rh–Rh 2 O 3) Nanostructures with Pt-like or Better Activity towards Hydrogen Evolution and Oxidation Reactions (HER, HOR) in Acid and Base. *J. Mater. Chem. A* **2018**, *6* (46), 23531–23541.

(5) Dan, Q.; Liao, F.; Sun, Y.; Zhang, S.; Huang, H.; Shen, W.; Kang, Z.; Shi, Y.; Shao, M. Rhodium/Silicon Quantum Dot/Carbon Quantum Dot Composites as Highly Efficient Electrocatalysts for Hydrogen Evolution Reaction with Pt-like Performance. *Electrochim. Acta* **2019**, *299*, 828–834.

(6) Duan, H.; Li, D.; Tang, Y.; He, Y.; Ji, S.; Wang, R.; Lv, H.; Lopes, P. P.; Paulikas, A. P.; Li, H.; et al. High-Performance Rh2P Electrocatalyst for Efficient Water Splitting. *J. Am. Chem. Soc.* **2017**, *139* (15), 5494–5502.

(7) Zhu, L.; Lin, H.; Li, Y.; Liao, F.; Lifshitz, Y.; Sheng, M.; Lee, S. T.; Shao, M. A Rhodium/Silicon Co-Electrocatalyst Design Concept to Surpass Platinum Hydrogen Evolution Activity at High Overpotentials. *Nat. Commun.* **2016**, *7*, 1–7.

(8) Zhang, N.; Shao, Q.; Pi, Y.; Guo, J.; Huang, X. Solvent-Mediated Shape Tuning of Well-Defined Rhodium Nanocrystals for Efficient Electrochemical Water Splitting. *Chem. Mater.* **2017**, *29* (11), 5009–5015.

(9) Wang, Y.; Liu, Z.; Liu, H.; Suen, N. T.; Yu, X.; Feng, L. Electrochemical Hydrogen Evolution Reaction Efficiently Catalyzed by Ru2P Nanoparticles. *ChemSusChem* **2018**, *11* (16), 2724–2729.